To understand the reflection process it is convenient to divide it into two steps. In the first step the photon is stopped (absorbed) by the reflecting surface and the photon's momentum is transferred to the vane. In the second step a photon is immediately emitted from the reflecting surface of the vane. By the principle of equal but opposite reaction a momentum equal to that of the emitted photon must be transferred to the vane during this second step. Therefore, it can be seen that the rotor must rotate so that the absorbing surface turns toward the radiation when opposite vanes are equally illuminated and equal in surface area.

It has been long known that Venus has a high albedo due to the scattering (similar to the reflection process) of solar radiation by the cloud droplets in its atmosphere. The radiation not scattered, but intercepted by the planet and its atmosphere, is mainly absorbed within the cloud layers. Therefore, momentum (equal, more or less, to that of the solar radiation intercepted) is continually transferred to the venusian atmosphere. An atmospheric system is different from the radiometer in that it presents a symmetrical surface (same radiation-matter interaction) toward the solar radiation at its morning and evening limbs (Fig. 3). If the cross-sectional areas at both limbs were equal as illustrated, the momentum transfer at the morning limb would decelerate the atmosphere's rotation while at the evening limb the same transfer would accelerate the rotation an equal amount. The net result of this is that the overall rate of rotation would be unchanged.

Such a symmetrical configuration is not likely since the atmosphere must be warmed as it rotates across the planet's day hemisphere and cooled as it rotates across the planet's night hemisphere. This warming and cooling must result in a formation of an asymmetrical configuration (Fig. 4). It is apparent that the momentum transfer at the evening limb must be greater than that at the morning limb because the atmosphere's greater cross section at the evening limb intercepts a greater amount of solar radiation. It should be noted that very little of the solar radiation is transmitted through the cloud layers, especially at or near the limbs where the atmospheric path length of the radiation is long. This net momentum transfer must be continually added to the angular momentum of the atmospheric system at the same time angular momentum is continually removed from the atmosphere by the frictional drag imposed on the atmosphere by the slowly rotating planet's surface. This completes the description of this mechanism.

There is great pressure to quantify the mechanism just introduced in an effort to evaluate its potential effectiveness. This pressure is resisted for the following reason. What physics professor would demonstrate the existence of radiation pressure and make the success or failure of the demonstration dependent upon the ability to predict the expected rate of rotation of an unknown apparatus? It is enough that the rotor turns in the direction predicted when the radiation source is set before the apparatus.
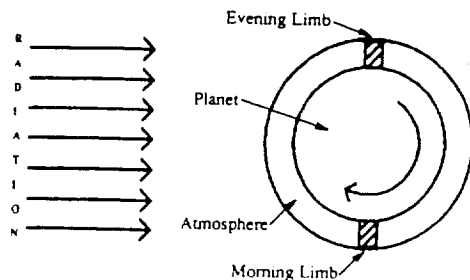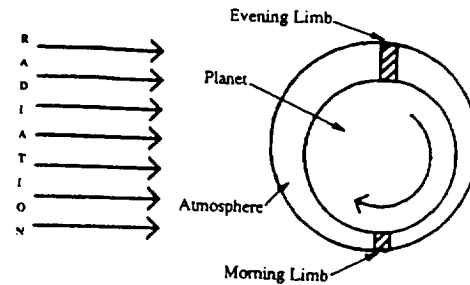

Fig. 4.   Atmosphere not to scale.

It should be enough that the qualitative details of the known superrotation of the venusian atmosphere are entirely consistent with the simple radiation pressure mechanism presented for this mechanism to receive serious consideration. An analysis of the frictional drag expected for the nearly laminar flow found beneath the cloud deck is much beyond my talent, to say nothing about the frictional coupling that exists in the turbulent cloud layer. It is possible that the mechanism might be tested if such frictional effects were reasonably well known.

The mechanism does suggest a possible phenomenon other than superrotation. The acceleration and deceleration that occur at the evening and morning limbs must compress the rotating atmosphere at some morning location and rarefy it at some afternoon location. A more detailed analysis of the expected atmospheric tides due to this mechanism is the subject of a nearly completed separate work.

A simple mechanism involving the phenomenon known as radiation pressure has been proposed to explain the superrotation of the venusian atmosphere. According to basic principles of physics it cannot be denied that the process must be active. It has been shown that support of the proposed mechanism by predictive, quantitative calculations is not presently possible because critical properties of the real system are unknown, or at best, poorly known. The possibility of atmospheric tides that, if observed, would be consistent with the mechanism has been noted. It should also be noted that the solar wind might replace the solar radiation in a similar mechanism. This has not been considered because the physics of the solar wind as it encounters a planet in its path is beyond my abilities.

Reference: [1] Belton M. J. S. et al. (1991) *Science, 253,* 1531–1536. (This article not only reports results from the Galileo venusian encounter, but also is a review of the superrotation phenomenon and is extensively referenced.)

LARGE-VOLUME LAVA FLOW FIELDS ON VENUS: DIMENSIONS AND MORPHOLOGY.

M. G. Lancaster[1], J. E. Guest[1], K. M. Roberts[2], and J. W. Head[2], [1]University of London Observatory, University College London, London NW7 2QS, UK, [2]Department of Geological Sciences, Brown University, Providence RI 02912, USA.

Of all the volcanic features identified in Magellan images, by far the most extensive and areally important are lava flow fields. Neglecting the widespread lava plains themselves, practically every C1-MIDR produced so far contains several or many discrete lava flow fields. These range in size from a few hundred square kilometers in area (like those fields associated with small volcanic edifices for example), through all sizes up to several hundred thousand

Fig. 3.   Atmosphere not to scale.

TABLE 1. Type examples of great flow fields. Areas are the total for each flow field, and the lengths and widths refer to flow units within each field.

Name	Latitude	Longitude	C1–MIDR	Area/km^2	Lengths/km	Widths/km	Morphology	Source
Lauma Dorsa	52N–67N	176–200	60n180 60n208	2,529,070	225–540	65–270	Sheet	Ridge belt
Aitra Mons	49N–54N	264–272	60n263 45n265	201,020	270 (aver.)	5–10	Symm. apron	Large volcano
Neago Fluctus	43N–59N	340–355	60n347 45n350	744,470	450–1900	90–450	Transitional	Fissures
Sekmet Mons	42N–50N	239–245	45n244	81,170	150–520	10–40	Asymm. apron	Large volcano
Mist Fossae	37N–43N	242–255	45n244	106,050	140–450	5–20	Subparallel	Rift zone
Kawelu Planitia	40N–52N	253–275	45n265	779,930	630 (max)	120–360	Sheet	Various
Ulfrun/Ganiki	24N–32N	215–223	30n225	197,550	670 (max)	20–45	Subparallel	Rift zone
Rusalka Planitia	10S–8N	170–185	00n180 15s180	773,470	280 (av.) 630 (max)	135 (typical)	Transitional	Various
Ozza Mons (S)	7S–2S	200–212	00n197 00n215	120,690	1460 (max)	35–130	Subparallel	Fissures
NW of Phoebe	1N–6N	266–273	00n266	137,730	260 (av.) 420 (max)	5–15	Apron	Large volcano
Parga Chasma	21S–13S	242–250	15s249	222,600	360 (av.) 632 (max)	≤20	Asymm. apron	Corona
Ammavaru	52S–43S	015–043	45s011 45s032	460,000	460 (fan) 880 (max)	≤30 (fan) ≤80 (ponds)	Fan	Caldera and shield cluster
Kaiwan Fluctus	53S–43S	353–010	45s011 45s350	≥315,000	870 (N) 1250 (max)	5–35	Subparallel	Fissures on rift zone
Mylitta Fluctus	63S–49S 43S	349–359	45s350 60s347	300,000	1000 (max)	5–80	Subparallel	Caldera on rift zone

square kilometers in extent (such as many rift related fields) [1]. Most of these are related to small, intermediate, or large-scale volcanic edifices, coronae, arachnoids, calderas [2,3], fields of small shields [4], and rift zones [5].

An initial survey of 40 well-defined flow fields with areas greater than 50,000 km^2 (an arbitrary bound) has been undertaken. Following Columbia River Basalt terminology, these have been termed great flow fields [6]. This represents a working set of flow fields, chosen to cover a variety of morphologies, sources, locations, and characteristics. The initial survey is intended to highlight representative flow fields, and does not represent a statistical set. For each flow field, the location, total area, flow lengths, flow widths, estimated flow thicknesses, estimated volumes, topographic slope, altitude, backscatter, emissivity, morphology, and source has been noted. The flow fields range from about 50,000 km^2 to over 2,500,000 km^2 in area, with most being several hundred square kilometers in extent. Flow lengths measure between 140 and 2840 km, with the majority of flows being several hundred kilometers long.

A few basic morphological types have been identified. This is not intended as a genetic classification, and the types identified are merely end members of a continuous range in morphology. The main distinction that has been drawn is between sheet flows, which are irregular in outline and show little or no internal structure, and digitate flows [7], which are made up of distinct flow lobes or lava streams. Usually, the digitate flows are related to a centralized

source, whereas the sheet flows were erupted from extensive fissures. The sheet flows cannot be divided into individual flow units and may therefore be termed simple flows [8], while the digitate flows, divisible into many flow units, are all compound (although individual flow units may be treated as simple).

Sheet flows are distinguished by their relatively uniform backscatter, lack of internal flow structure such as well-defined lava streams, channels, etc., absence of flow lobes, and irregular boundaries. Of the studied set, they range from 66,210 km^2 to 2,529,070 km^2. Sheet widths lie between 60 to 360 km, with maximum lengths between 225 and 680 km. The sheet flow fields are difficult to map in the sense that internal flow boundaries are essentially absent. Source regions for sheet flows are typically the fissures associated with rift zones, but they may also be traced to the annular structures surrounding some coronae. Some of the larger sheet flow fields may conceivably be composed of more than one large flow field.

Digitate flow fields are characterized by many discrete flow lobes or lava streams. They are more common, and show a wider range of morphology than sheet flows. Relative to sheet flow fields they display a wider variation in radar backscatter, often being composed of both radar-bright and -dark flow units within the same field. They have been subdivided into divergent and subparallel morphologies on the basis of the distal widening of the overall flow field and the downstream divergence between flow units. All the divergent flow fields have central sources, whereas half the subparallel fields have been erupted from fissures along sections of
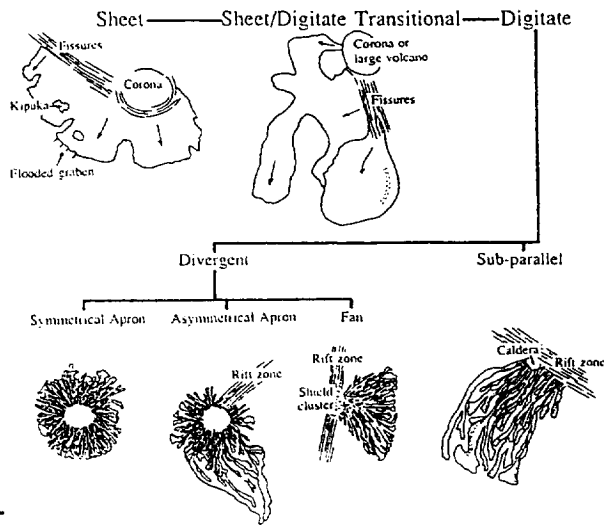
Fig. 1. Morphological types of great flow fields (not to scale).

rift zone. The more centered the source, the greater the degree of divergence of the flow field, although the local topography may also control the direction of flow lobes. The divergent fields contain symmetrical apron and fan end members. However, a large number of aprons are distinctly asymmetric in plan, and may be considered transitional between symmetrical aprons and fans. All the symmetrical aprons surround large volcanos, while the asymmetrical aprons are centered on large volcanos (some of which are on rift zones), coronae, and a cluster of small shields. Of the studied fans, two are related to shield clusters, while a third may be traced to a set of fissures. Fans are the least common of all the surveyed fields. The subparallel fields may be traced to rift zones and fissures, coronae, calderas, and a cluster of small shields.

In all types the widths of individual flow lobes or streams ranges from a few kilometers (usually in the proximal regions) to several tens of kilometers, with distal lobes of asymmetric aprons and subparallel flow fields up to 130 km in width. The symmetrical aprons are typically around 300 km in radius, while the maximum length of the asymmetric aprons are up to 770 km in maxiumum length. The measured subparallel flow fields range between 140 and 1460 km in length, with typical lengths of a few hundred kilometers. Most of the symmetrical and assymetrical aprons have relatively radar-bright proximal regions, while many of the asymmetrical aprons have distal regions of particularly low backscatter. All the divergent types may display channels.

A number of flow fields are transitional between the sheet and digitate types. In these cases, very broad, but sheetlike flow lobes, up to a few hundred kilometers across, may be discriminated. These large lobes tend to have somewhat more variable backscatter than the sheet flows. In several cases these transitional flows appear to consist of large expanses of ponded lava. The transitional flows are all associated with fissures. The plains contain numerous examples of portions of flow fields that cannot be traced to their source. These flows are usually indistinct, and may represent relatively old, degraded flows that have been partly resurfaced by later volcanism. Such indistinct flows occur beyond the distal reaches of some large flow fields such as Mylitta Fluctus [7] and Kaiwan Fluctus [1]. A key question regarding the great flow fields is how they relate to plains development and what their contribution is to volcanic

resurfacing in general [9]. Another key question concerns the effusion rates and emplacement times for these great flows, as has been estimated for Mylitta Fluctus [7]. The set of flow fields has been chosen to address these questions, with initial emphasis (mapping, detailed measurements, etc.) being placed on the type flow fields.

References: [1] Lancaster M. G. et al. (1992) *LPSC XXIII*, 753–754. [2] Crumpler L. S. et al. (1992) *LPSC XXIII*, 277–278. [3] Head J. W. et al. (1992) *LPSC XXIII*, 513–514. [4] Aubele J. C. et al. (1992) *LPSC XXIII*, 47–48. [5] Roberts K. M. et al. (1992) *LPSC XXIII*, 1157–1158. [6] Tolan T. L. et al. (1989) In *Volcanism and Tectonism in the Columbia River Flood-Basalt Province, Boulder, Colorado* (S. P. Reidel and P. R. Hooper, eds.), GSA Spec. Paper 239. [7] Roberts K. M. et al. (1992) *JGR*, special Magellan issue, submitted. [8] Walker G. P. L. (1971) *Bull. Volcanol.*, *XXXV-3*, 579–590. [9] Head J. W. et al. (1992) *LPSC XXIII*, 517–518.

N93-14340

DERIVATION OF SURFACE PROPERTIES FROM MAGELLAN ALTIMETRY DATA.

Amy J. Lovell[1], F. Peter Schloerb[1], and George E. McGill[2],[1]Department of Physics and Astronomy, University of Massachusetts, Amherst MA 01003, USA, [2]Department of Geology and Geography, University of Massachusetts, Amherst MA 01003, USA.

The fit of the Hagfors model [1] to the Magellan altimetry data provides a means to characterize the surface properties of Venus. However, the derived surface properties are only meaningful if the model provides a good representation of the data. The Hagfors model is generally a realistic fit to surface scattering properties of a nadir-directed antenna [2] such as the Magellan altimeter; however, some regions of the surface of Venus are poorly described by the existing model, according to the "goodness of fit" parameter provided on the ARCDR CDRoms. Poorly characterized regions need to be identified and fit to new models in order to derive more accurate surface properties for use in inferring the geological processes that affect the surface in those regions.

We have compared the goodness of fit of the Hagfors model to the distribution of features across the planet, and preliminary results show a correlation between steep topographic slopes and poor fits to the standard model, as has been noticed by others [3,4]. In this paper, we investigate possible relations between many classes of features and the ability of the Hagfors model to fit the observed echo profiles. In the regions that are not well characterized by existing models, we calculate new models that compensate for topographic relief in order to derive improved estimates of surface properties.

Areas investigated to date span from longitude 315 through 45, at all latitudes covered by Magellan. A survey of those areas yields preliminary results that suggest that topographically high regions are well suited to the current implementation of the Hagfors model. Striking examples of such large-scale good fits are Alpha Regio, the northern edges of Lada Terra, and the southern edge of Ishtar Terra. Other features that are typically well fit are the rims of coronae such as Heng-O and the peaks of volcanos such as Gula Mons. Surprisingly, topographically low regions, such as the ubiquitous plains areas, are modeled poorly in comparison. However, this generalization has exceptions: Lakshmi Planum is an elevated region that is not well fit compared to the rest of neighboring Ishtar, while the southern parts of topographically low Guinevere Planitia are characterized quite well by the Hagfors model.

Features that are candidates for improved models are impact craters, coronae, ridges of significant scale, complex ridged ter-